PKN1 controls the aggregation, spheroid formation, and viability of mouse embryonic fibroblasts in suspension culture

Mehruba, Mona

Siddique, Salman Mahmud

Mukai, Hideyuki

(Citation)
Biochemical and Biophysical Research Communications,523(2):398-404

(Issue Date)
2020-03

(Resource Type)
journal article

(Version)
Accepted Manuscript

(URL)
https://hdl.handle.net/20.500.14094/90007066

PKN1 controls the aggregation, spheroid formation, and viability of mouse embryonic fibroblasts in suspension culture

Mona Mehruba[a], Salman Mahmud Siddique[a], Hideyuki Mukai[a,b,*]

[a]Graduate School of Medicine, Kobe University, Kobe, 650-0017, Japan

[b]Biosignal Research Center, Kobe University, Kobe, 657-8501, Japan

Abbreviations:

MEF,mouse embryonic fibroblast; WT,wild type; PKN1[T778A], PKN1 T778A/T778A homozygous knock-in; poly-HEMA, poly-2-hydroxyethylmethacrylate; rpm, revolutions per minute; MFI, mean fluorescent intensity

*Corresponding author:

Email address: mukinase@kobe-u.ac.jp

Biosignal Research Center, Kobe University, 1-1 Nada, Kobe 657-8501, Japan

Abstract

The role of protein kinase N1 (PKN1) in cell aggregation and spheroid formation was investigated using mouse embryonic fibroblasts (MEFs) deficient in kinase activity caused by a point mutation (T778A) in the activation loop. Wild type (WT) MEFs formed cell aggregates within a few hours in suspension cultures placed in poly-2-hydroxyethylmethacrylate (poly-HEMA) coated flat-bottom dishes. By contrast, PKN1[T778A] (PKN1 T778A/T778A homozygous knock-in) MEFs showed significantly delayed aggregate formation and higher susceptibility to cell death. Video analysis of suspension cultures revealed decreased cell motility and lesser frequency of cell-cell contact in PKN1[T778A] MEFs compared to that in WT MEFs. Aggregate formation of PKN1[T778A] MEFs was compensated by shaking the cell suspension. When cultured in U-shaped ultra-low attachment well plates, initially larger-sized and loosely packed aggregates of WT MEFs underwent compaction resulting in a single round spheroid. On the other hand, image-based quantitative analysis of PKN1[T778A] MEFs revealed irregular compaction with decreased roundness, solidity, and sphericity within 24 hours. Flow cytometry of PKN1[T778A] MEFs revealed decreased surface-expression of N-cadherin and integrins α5 and αV. These results suggest that kinase activity of PKN1 controls cell aggregation and spheroid compaction in MEF suspension culture, possibly by regulating the cell migration and cell-surface expression of N-cadherin and integrins.

Keywords

Key words: spheroid, fibroblast, cadherin, integrin, protein kinase, anoikis

Introduction

Cell aggregate/spheroid culture is one of the 3D cell culture methods which are regarded to provide clinical and biological relevance to *in vitro* experiments. The observed differences between cell aggregate/spheroid and 2D cultures are mainly due to differential cell–cell and cell–matrix interactions [1]. Many types of mammalian cells can aggregate and differentiate into multicellular spheroids when cultured in suspension or in a non-adhesive environment. Multicellular spheroids formed by transformed cells are widely used as avascular tumor models for metastasis and invasion studies. On the other hand, multicellular spheroids formed by primary cells show enhanced viability. Particularly, fibroblast spheroids formed *in vitro* are activated to produce massive amounts of cyclooxygenase-2, prostaglandins, proteinases, proinflammatory cytokines, and growth factors [2-7]. It is speculated that similar instances occur *in vivo* since proteases destroy connective tissue during inflammation, cancer, and wound healing, liberating fibroblasts from the extracellular matrix and leading them to aggregate together. Therefore, cell aggregate/spheroid cultures of fibroblasts *in vitro* are regarded as practical models for various pathological conditions. However, the exact mechanism of cell aggregate/spheroid formation has not been fully elucidated.

Protein kinase N (PKN) is a serine/threonine protein kinase with a catalytic domain homologous to protein kinase C (PKC) and a regulatory region containing antiparallel coiled-coil (ACC) finger domains [8]. PKN1, also known as PKNα or PRK1, is one of the three PKN isoforms (PKN1, PKN2, and PKN3) derived from different genes in mammals [8]. PKN1 is an effector protein kinase of the Rho family GTPases, such as RhoA, RhoB, RhoC, and Rac1, in mammalian tissues [9-12]. Rho family GTPases play an important role as regulators of cell-cell adhesion in a manner which varies substantially depending on cell type and cellular context [13,14]. PKN1 is also involved in cell-cell adhesion among mammary epithelial cells [15] and in lymphocyte adhesion to vascular endothelial cells [16], whereas direct interactions between PKN1 and Rho family GTPases were not described in these cases.

In this study, we prepared MEFs from PKN1[T778A] mice deficient in PKN1 kinase activity due to the introduction of a point mutation (T778A) in the enzyme's activation loop [17] and examined whether PKN1 is involved in cell aggregate/spheroid formation of fibroblasts *in vitro*.

Material and methods

Preparation of MEFs

MEFs were obtained from 14.5-day-old embryos of PKN1[T778A] mice and control WT mice as described previously [18]. Primary fibroblasts were cultured in Dulbecco's Modified Eagle Medium (DMEM; Nacalai Tesque, Inc., Kyoto, Japan) supplemented with 10% Gibco Fetal Bovine Serum (Gibco FBS; Thermo Fisher Scientific, Waltham, MA, USA) at 37°C and 5% CO_2 level in the CO_2 incubator.

Morphological analysis of MEFs

MEFs were placed in normal culture dishes or poly-HEMA coated flat-bottom dishes and images were taken at indicated time points using BZ-9000 All-in-one Fluorescence Microscope (Keyence Corporation, Osaka, Japan). Number and area of all cell aggregates per well of 96 well plates were measured using ImageJ software. Time-lapse video microscopy was performed in poly-HEMA coated flat-bottom well plate equipped with environmental chamber to keep 37°C and 5% CO_2 level. Ten random cells each from WT and PKN1[T778A] MEFs were tracked, and distance and velocity of cell migration were measured per experiment by ImageJ software, which was repeated three times. To artificially increase cell motility, the suspension cultures in poly-HEMA coated flat-bottom well plate were shaken at 60, 120, and 180 revolutions per minute (rpm). Spheroid morphologies such as roundness, solidity, and sphericity index were analyzed in U-shaped ultra-low-attachment (Prime Surface) well plates using ImageJ software as previously described [19].

Viability assay

DNA quantification was performed using CyQUANT® Cell Proliferation Assay Kit (Molecular Probes/Invitrogen, Waltham, MA, USA) following the manufacturer's instruction. Fluorescence intensity was measured using Synergy™ HTX Multi-Mode Microplate Reader

(BioTek Japan, Tokyo, Japan) with Gen5™ software at a wavelength of 485 nm for excitation and 528 nm for emission. ATP content was quantified using Cell-Titer Glo® 3D Cell Viability Assay Kit (Promega, Madison, WI, USA) following the manufacturer's protocol. Luminescence was also monitored using the same microplate reader. Three samples per condition (n=3) were considered for each analysis.

Flow cytometry

The monoclonal antibodies used for flow cytometric analysis of cell-surface antigens were allophycocyanin (APC)-conjugated anti-mouse CD49e (integrin α5; clone 5H10-27), APC-conjugated anti-mouse/rat CD29 (integrin β1; clone HMβ1-1), phycoerythrin-conjugated anti-mouse CD51 (integrin αV; clone RMV-7; BioLegend, San Diego, CA, USA), and Alexa Fluor® 488 conjugated N-Cadherin Antibody (Clone 8C11; Novus Biologicals, Centennial, CO, USA). MEFs were resuspended in staining buffer (0.5% bovine serum albumin in Hanks' Balanced Salt Solution with 25 mM HEPES, pH 7.5, 5 mM ethylenediaminetetraacetic acid, and 0.1% sodium azide) and labeled with appropriate primary antibodies for 30 minutes on ice. After washing with staining buffer, MEFs were incubated with **7**-amino-actinomycin D for 15 minutes at room temperature and analyzed by flow cytometry using an Accuri™ system (BD Biosciences, Franklin Lakes, NJ, USA). Data were analyzed using BD Accuri™ C6 software (BD Biosciences, Franklin Lakes, NJ, USA) and FlowJo (Tree Star, Inc., Ashland, OR, USA).

Statistical analysis

Data presented in the figures and text represent mean ± SEM of independent experiments. Statistical significance was calculated using *t*-test or repeated measures ANOVA with P value < *0.05* indicated in the figure legends..

Data Availability

The datasets generated and/or analyzed during the current study are available from the corresponding author on reasonable request.

Results and discussion

PKN1[T778A] MEFs show delayed aggregate formation in suspension culture in poly-HEMA coated flat-bottom dishes and wells of plates

Phase-contrast microscopy of cells in normal attachment culture conditions did not show significant difference in morphology between WT and PKN1[T778A] MEFs (Fig. 1A). Suspension cultures of WT MEFs in flat-bottom poly-HEMA coated dishes time-dependently formed cell aggregates within a few hours (Fig. 1B). On the other hand, PKN1[T778A] MEFs showed significantly delayed aggregation in suspension cultures. Additionally, PKN1[T778A] MEFs aggregates formed within 24 hours had smaller number and area compared with WT MEFs (Fig. 1C and 1D). To investigate the cause of delayed aggregation, we analyzed cell behavior by video imaging from 10 minute after plating in poly-HEMA coated flat-bottom wells of plates (video_WT and video_T778A). The average velocity and distance covered of each cell were significantly reduced in PKN1[T778A] MEFs than in WT MEFs (Fig. 1E and 1F). Cell-cell contact in PKN1[T778A] MEFs occurred less frequently compared with WT MEFs (video_WT and video_T778A). Thus, we artificially increased the frequency of cell-cell contact by shaking the cell cultures in a graded manner. Suspension cultures of PKN1[T778A] MEFs shaken at 60 rpm still failed to form aggregates (Fig. 1G). By increasing the speed from 60 to 120 rpm, PKN1[T778A] MEFs came in close contact with each other and finally formed aggregates like WT MEFs at 180 rpm for 1 hour. Results suggest that less frequency of cell-cell contact due to impaired cell motility contributes to the delayed aggregate formation of PKN1[T778A] MEFs in suspension culture. It was previously reported that PKN1 controls cell migration of cancer cells such as bladder and prostate tumor cells in attachment culture condition [20,21]. Our study suggests that PKN1 controls motility of primary fibroblasts that leads to early cell aggregate formation even in suspension culture condition.

PKN1[T778A] MEFs show susceptibility to anoikis in suspension culture

Normal non-hematopoietic cells typically undergo rapid cell death once attachments to the extracellular matrix are lost via anoikis (i.e., detachment-induced apoptosis) [22]. Thus, we examined whether inactivation of PKN1 in MEFs affect cell viability in suspension culture in poly-HEMA coated flat-bottom well of plate. Cell viability was evaluated by quantifying the DNA content using a fluorescence-based method and the cellular ATP level using a luminescence-based method [23]. Both DNA and ATP contents increased time-dependently in parallel for both WT and PKN1[T778A] MEFs under attachment culture condition (Fig. 2A and 2B), suggesting no difference in the cell viability between the two. However, both DNA and ATP contents decreased time-dependently in parallel for both WT and PKN1[T778A] MEFs in suspension cultures in poly-HEMA coated flat-bottom wells of plates (Fig. 2C and 2D), suggesting that both underwent cell death. Particularly, PKN1[T778A] MEFs had significantly less DNA and ATP contents, suggesting that these were more susceptible to cell death than WT MEFs. These results imply that PKN1 activity contributes to resistance to anoikis. Previous reports stated that anoikis can be suppressed through cell-cell adhesion by a variety of cells [24,25]. Therefore, the delayed cell aggregation observed in PKN1[T778A] MEFs may be causing the higher susceptibility to cell death in suspension culture.

PKN1[T778A] MEFs show impaired compaction for spheroid formation in suspension culture

Generation of a multicellular spheroid of fibroblasts in suspension culture has been described as a stepwise process. It starts from the initial loose aggregation of dispersed cells and transitions toward the formation of tight spheroids, i.e. compaction stage [26]. We observed delayed initial aggregate formation in PKN1[T778A] MEFs due to decreased motility in suspension culture as described above. To examine if PKN1 is involved in the compaction stage of MEFs, we used U-shaped ultra-low-attachment (Prime Surface) well plates that reportedly support growth and formation of tight spheroids or compact aggregates in a variety of cell lines [27]. Initially larger-sized and loosely packed WT MEF aggregates underwent time-dependent

compaction into a single round spheroid (Fig. 3A). However, PKN1[T778A] MEFs revealed irregular compaction with significantly less roundness, solidity, and sphericity than WT MEFs before 24 hours and only formed the compact spheroid like WT MEFs after 48 hours (Fig. 3B). This suggests that PKN1 is required for the formation of regularly shaped spheroid during compaction stage but not for the resultant compact spheroid of MEFs. We also examined if PKN1 is involved in cell viability during the compaction process in U-shaped ultra-low-attachment well plates. PKN1[T778A] MEFs has significantly decreased ATP content than WT MEFs (Fig. 3C), suggesting that PKN1[T778A] MEFs are more susceptible to cell death during compaction stage.

Surface expression of N-cadherin and integrins α5 and αV are downregulated in PKN1[T778A] MEFs

Cadherin is one of the most critical molecules responsible for the formation and maintenance of cell-cell contact. Previous studies using blocking antibodies against E-cadherin revealed that E-cadherin is critical in the formation of multicellular spheroids of various cell lines (e.g., renal cancer cell lines SKRC6, 59, and RT4 [28]; colon cancer cell line HT29, lung cancer cell line L23, breast cancer cell line BT20 [29]; breast cancer cell lines MCF7, BT-474, T-47D, and MDA-MB-361 [30]; Ewing sarcoma cell lines TC32 and TC71[24]; mammary cancer cell lines HC11 and 4T1, and mammary epithelial cell line T47D [31], and hepatoma line HepG2 [32]). N-cadherin was also demonstrated to be responsible for aggregate/spheroid formation, specifically in cell lines expressing very low E-cadherin levels (e.g., breast cancer cell line MDA-MB-435S [30], embryonic kidney cell line HEK293T cells [33], and renal cancer cell line SKRC-52 [28]), using blocking antibodies against N-cadherin or siRNA-mediated N-cadherin knockdown. Both WT and PKN1[T778A] MEFs expressed almost undetectable levels of E-cadherin by immunoblotting (data not shown), corroborating the report stating that fibroblasts express N-cadherin, whereas E- and P-cadherins are undetectable [34]. Thus, we compared the surface expression of N-cadherin

on WT and PKN1[T778A] MEFs collected 30 minutes after starting suspension culture using flow cytometry. Surface N-cadherin expression level evaluated by mean fluorescent intensity (MFI) was significantly lower in PKN1[T778A] MEFs than WT MEFs (Fig. 4A and 4B). Tachibana previously reported that siRNA-mediated N-cadherin knockdown in HEK293T cells induces protrusion at the surface of aggregates, suggesting an essential function of N-cadherin in the formation of tightly packed aggregates/spheroids as well as early cell aggregation [33]. Considering that the irregularly shaped spheroid was observed in PKN1[T778A] MEFs (Fig. 3A and 3B), the lower expression of N-cadherin may be causing the abnormal aggregate/spheroid formation of PKN1[T778A] MEFs in suspension culture.

Fibronectin is a major extracellular matrix product of fibroblasts responsible for the formation of multicellular spheroid of fibroblasts; hence, fibronectin-knockout fibroblasts do not form compact spheroids [26]. Integrins α5, αV, and β1 are fibronectin-binding integrin subunits highly-expressed in fibroblasts. It was also reported that fibroblasts treated with anti-β1 and anti-α5 antibodies formed loose spheroids [26]. Thus, we examined the surface expression of integrins α5, αV, and β1 on MEFs using flow cytometry. MFI of integrins α5 and αV were significantly lower in PKN1[T778A] MEFs than WT MEFs (Fig. 4A and 4B). Therefore, the decreased surface expression of integrins may also contribute to the abnormal aggregate/spheroid formation of PKN1[T778A] MEFs.

What is the potential mechanism underlying the decrease in surface expression of N-cadherin and integrins by inactivation of PKN1? Some part of PKN1 molecules are localized to vesicles and involved in vesicular trafficking of several transmembrane proteins such as the EGF receptor [35], LRP6 [36], and Glut4 [37]. Integrins are also transmembrane proteins constantly trafficked in cells and internalized via endocytosis. A large portion of integrins is recycled back to the plasma membrane since these can potentially bypass the protein downregulation machinery [38]. Yuan et al. reported that PKN1 regulates trafficking of small GTPase Rab21-positive vesicles via phosphorylation of RPH3A, a Rab21 effector, leading to the localization of

PIP5K1C90 on the plasma membrane of neutrophils [16]. Rab21 is also known to be involved in integrin recycling [38], wherein β2-integrin exhibits polarized localization to the plasma membrane in fibronectin-stimulated neutrophils, while β2-integrin polarization is impaired in PKN1 or RPH3A-deficient neutrophils [16]. Therefore, decreased surface expression of integrin α5 and αV in PKN1[T778A] MEFs might be due to the reduced recycling of Rab21-positive vesicles due to PKN1-induced RPH3A phosphorylation deficiency. N-cadherin is also a transmembrane protein cell surface level of which is thought to be dynamically regulated through new protein synthesis, endocytosis, recycling, and degradation [39]. Thus, the low surface expression of N-cadherin in PKN1[T778A] MEFs might also be due to impaired vesicle trafficking caused by PKN1 inactivation. However, the detailed molecular mechanism of N-cadherin trafficking has not been fully explained. Calautti et al. previously reported that E-cadherin localization at cell-cell border in keratinocytes can be induced via tyrosine phosphorylation of catenin by Fyn, while Fyn activation is induced by PKN1/2 downstream of the active Rho GTPase [40]. Hence, N-cadherin localization might also be regulated by catenin phosphorylation downstream of PKN1.

PKN1 has been regarded as a promising target for cancer treatment based on its role in transcription and cell migration activity; hence, PKN1 kinase inhibitors have already been developed for therapeutic purposes [41,42]. Therefore, it would be beneficial to discover the biological consequences of PKN1 inhibition in various tissues. This study focused on the effect of PKN1 inactivation in aggregate/spheroid formation of primary fibroblasts, which are regarded as practical models *in vitro* for pathological conditions such as cancer and inflammation. Further investigation regarding the effect of PKN1 inactivation on the activity of aggregate/spheroid of fibroblasts (e.g. production of cytokines, growth factors, and proteases) may help elucidate a new mode of action and the therapeutic or adverse effects of PKN1 inhibitors.

Conflict of interest

The authors declare no competing interests.

Acknowledgements

We thank Koji Kubouchi for his help with the experiments and his valuable ideas for the discussion. We also thank Editage for the English language editing. This study was supported by research grants from the Ministry of Education, Culture, Sports, Science and Technology, Japan.

Figure Legends

Fig. 1. PKN1[T778A] MEFs show delayed aggregate formation compared with WT MEFs in suspension culture in poly-HEMA coated flat-bottom dish and well of plate.

WT and PKN1[T778A] MEFs plated (A) in normal culture dish and (B) in poly-HEMA coated flat-bottom dish. Phase contrast images were taken after 2, 5, and 24 hours (10X magnification, scale bar = 300 μm). h, hour.

(C) The number and (D) average area of cell aggregates in WT (open bar) and PKN1[T778A] (closed bar) MEFs formed in suspension cultures in poly-HEMA coated flat-bottom wells of plates after 2, 5, and 24 hours (n = 3). Data were analyzed using repeated measures ANOVA (*P < *0.05*). h, hour.

(E) Cell migration velocity and (F) distance of WT (open circle) and PKN1[T778A] (closed circle) MEFs in suspension cultures in poly-HEMA coated flat-bottom wells of plates. Cells were tracked for the first 20 minutes at one minute intervals (n = 30). Data were analyzed using unpaired t-test (***P < *0.001*).

(G) Phase contrast images of WT and PKN1[T778A] MEFs in suspension cultures in poly-HEMA coated flat-bottom 96 well plate cultured with shaking for one hour at 60, 120, and 180 rpm (10X magnification, scale bar = 300 μm).

Fig. 2. Cell viability is reduced in PKN1[T778A] than WT MEFs in suspension culture (n = 3). Data were analyzed by repeated measures ANOVA (*P < *0.05*, **P < *0.01*). h, hour.

DNA contents of WT (open bar) and PKN1[T778A] (closed bar) MEFs (A) in attachment cultures and (C) in suspension cultures in poly-HEMA coated flat-bottom well plate quantified using fluorescence-based assay.

ATP contents of WT (open bar) and PKN1[T778A] (closed bar) MEFs (B) in attachment cultures and (D) in suspension cultures in poly-HEMA coated flat-bottom well plate quantitated using luminescence-based assay.

Fig. 3. PKN1[T778A] MEFs show impaired spheroid compaction in suspension culture.

h, hour.

(A) Phase contrast images of WT and PKN1[T778A] MEFs plated in U-shaped ultra-low-attachment well plate taken after 1, 2, 5, 10, 24, and 48 hours (10X magnification, scale bar = 300 μm).

(B) Roundness, solidity, and sphericity index of spheroids from WT (open circle) and PKN1[T778A] (closed circle) MEFs in U-shaped ultra-low-attachment well plate. The roundness indicates the circularity of the projected area of the spheroids, the solidity indicates the regularity of spheroids surface, and the sphericity index determines how close to a spherical geometry shape the samples are [19] (n = 3). Data were analyzed using repeated measures ANOVA. Roundness, P = 0.03; solidity, P = 0.04; sphericity index, P = 0.04.

(C) ATP contents of WT (open bar) and PKN1[T778A] (closed bar) MEFs in suspension cultures in U-shaped ultra-low-attachment well plate after 1, 5, 10, 24, and 48 hours (n = 3). Data were analyzed using repeated measures ANOVA (*P < *0.05*).

Fig. 4. N-cadherin and integrins α5 and αV are downregulated in PKN1[T778A] MEFs.

(A) Flow cytometric analysis of the surface expression of N-cadherin and integrin α5, αV, and β1 subunits in WT (dashed line) and PKN1[T778A] (solid line) MEFs. Representative data is shown in histogram. (B) Significance was determined by comparing mean fluorescence intensities. Data from WT (open circle) and PKN1[T778A] MEFs (closed circle) obtained on the same day are connected by a solid line. Data were analyzed using paired t-test (n = 5; *P < *0.05*, **P < *0.01*).

Video_WT and video_ T778A. Time lapse videos showing the cell aggregation of WT (video_WT.avi) and PKN1[T778A] (video_T778A.avi) MEFs in suspension cultures (in poly-

HEMA coated flat-bottom well plate). Videos with a duration of one hour each were taken 10 minutes after plating the cells.

<References>

[1] E. Fennema, N. Rivron, J. Rouwkema, et al., Spheroid culture as a tool for creating 3D complex tissues, Trends in Biotechnology 31 (2013) 108-115.

[2] J. Bizik, E. Kankuri, A. Ristimaki, et al., Cell-cell contacts trigger programmed necrosis and induce cyclooxygenase-2 expression, Cell Death Differ 11 (2004) 183-195.

[3] E. Kankuri, D. Cholujova, M. Comajova, et al., Induction of hepatocyte growth factor/scatter factor by fibroblast clustering directly promotes tumor cell invasiveness, Cancer Res. 65 (2005) 9914-9922.

[4] A. Enzerink, P. Salmenpera, E. Kankuri, et al., Clustering of fibroblasts induces proinflammatory chemokine secretion promoting leukocyte migration, Molecular Immunology 46 (2009) 1787-1795.

[5] A. Enzerink, V. Rantanen, A. Vaheri, Fibroblast nemosis induces angiogenic responses of endothelial cells, Exp. Cell Res. 316 (2010) 826-835.

[6] E. Kankuri, O. Babusikova, K. Hlubinova, et al., Fibroblast nemosis arrests growth and induces differentiation of human leukemia cells, Int. J. Cancer 122 (2008) 1243-1252.

[7] V. Siren, P. Salmenpera, E. Kankuri, et al., Cell-cell contact activation of fibroblasts increases the expression of matrix metalloproteinases, Ann Med 38 (2006) 212-220.

[8] H. Mukai, The structure and function of PKN, a protein kinase having a catalytic domain homologous to that of PKC, J Biochem 133 (2003) 17-27.

[9] G. Watanabe, Y. Saito, P. Madaule, et al., Protein kinase N (PKN) and PKN-related protein rhophilin as targets of small GTPase Rho, Science 271 (1996) 645-648.

[10] M. Amano, H. Mukai, Y. Ono, et al., Identification of a putative target for Rho as the serine-threonine kinase protein kinase N, Science 271 (1996) 648-650.

[11] D. Owen, P.N. Lowe, D. Nietlispach, et al., Molecular dissection of the interaction between the small G proteins Rac1 and RhoA and protein kinase C-related kinase 1 (PRK1), J Biol Chem 278 (2003) 50578-50587.

[12] N.E. Torbett, A. Casamassima, P.J. Parker, Hyperosmotic-induced protein kinase N 1 activation in a vesicular compartment is dependent upon Rac1 and 3-phosphoinositide-dependent kinase 1, J Biol Chem 278 (2003) 32344-32351.

[13] A. Hall, Rho GTPases and the actin cytoskeleton, Science 279 (1998) 509-514.

[14] M. Fukata, K. Kaibuchi, Rho-family GTPases in cadherin-mediated cell-cell adhesion, Nat. Rev. Mol. Cell Biol. 2 (2001) 887-897.

[15] A. Fischer, H. Stuckas, M. Gluth, et al., Impaired tight junction sealing and precocious involution in mammary glands of PKN1 transgenic mice, J Cell Sci 120 (2007) 2272-2283.

[16] Q. Yuan, C. Ren, W. Xu, et al., PKN1 Directs Polarized RAB21 Vesicle Trafficking via RPH3A and Is Important for Neutrophil Adhesion and Ischemia-Reperfusion Injury, Cell reports 19 (2017) 2586-2597.

[17] R. Mashud, A. Nomachi, A. Hayakawa, et al., Impaired lymphocyte trafficking in mice deficient in the kinase activity of PKN1, Sci Rep 7 (2017) 7663.

[18] S. Danno, K. Kubouchi, M. Mehruba, et al., PKN2 is essential for mouse embryonic development and proliferation of mouse fibroblasts, Genes Cells 22 (2017) 220-236.
[19] R.L.F. Amaral, M. Miranda, P.D. Marcato, et al., Comparative Analysis of 3D Bladder Tumor Spheroids Obtained by Forced Floating and Hanging Drop Methods for Drug Screening, Front Physiol 8 (2017) 605.
[20] S. Lachmann, A. Jevons, M. De Rycker, et al., Regulatory domain selectivity in the cell-type specific PKN-dependence of cell migration, PLoS One 6 (2011) e21732.
[21] C.A. Jilg, A. Ketscher, E. Metzger, et al., PRK1/PKN1 controls migration and metastasis of androgen-independent prostate cancer cells, Oncotarget 5 (2014) 12646-12664.
[22] S.M. Frisch, R.A. Screaton, Anoikis mechanisms, Current opinion in cell biology 13 (2001) 555-562.
[23] A.L. Niles, R.A. Moravec, T.L. Riss, In vitro viability and cytotoxicity testing and same-well multi-parametric combinations for high throughput screening, Curr Chem Genomics 3 (2009) 33-41.
[24] H.G. Kang, J.M. Jenabi, J. Zhang, et al., E-cadherin cell-cell adhesion in ewing tumor cells mediates suppression of anoikis through activation of the ErbB4 tyrosine kinase, Cancer Res 67 (2007) 3094-3105.
[25] C. Hofmann, F. Obermeier, M. Artinger, et al., Cell-cell contacts prevent anoikis in primary human colonic epithelial cells, Gastroenterology 132 (2007) 587-600.
[26] P. Salmenpera, E. Kankuri, J. Bizik, et al., Formation and activation of fibroblast spheroids depend on fibronectin-integrin interaction, Exp Cell Res 314 (2008) 3444-3452.
[27] M. Vinci, S. Gowan, F. Boxall, et al., Advances in establishment and analysis of three-dimensional tumor spheroid-based functional assays for target validation and drug evaluation, BMC Biol 10 (2012) 29.
[28] T. Shimazui, J.A. Schalken, K. Kawai, et al., Role of complex cadherins in cell-cell adhesion evaluated by spheroid formation in renal cell carcinoma cell lines, Oncol Rep 11 (2004) 357-360.
[29] B. St Croix, C. Sheehan, J.W. Rak, et al., E-Cadherin-dependent growth suppression is mediated by the cyclin-dependent kinase inhibitor p27(KIP1), J Cell Biol 142 (1998) 557-571.
[30] A. Ivascu, M. Kubbies, Diversity of cell-mediated adhesions in breast cancer spheroids, Int J Oncol 31 (2007) 1403-1413.
[31] I. Smyrek, B. Mathew, S.C. Fischer, et al., E-cadherin, actin, microtubules and FAK dominate different spheroid formation phases and important elements of tissue integrity, Biol Open 8 (2019).
[32] R.Z. Lin, L.F. Chou, C.C. Chien, et al., Dynamic analysis of hepatoma spheroid formation: roles of E-cadherin and beta1-integrin, Cell Tissue Res 324 (2006) 411-422.
[33] K. Tachibana, N-cadherin-mediated aggregate formation; cell detachment by Trypsin-EDTA loses N-cadherin and delays aggregate formation, Biochem Biophys Res Commun 516 (2019) 414-418.
[34] A.T. Ho, E.B. Voura, P.D. Soloway, et al., MMP inhibitors augment fibroblast adhesion through stabilization of focal adhesion contacts and up-regulation of cadherin function, J Biol Chem 276 (2001) 40215-40224.
[35] A. Gampel, P.J. Parker, H. Mellor, Regulation of epidermal growth factor receptor traffic by the small

GTPase rhoB, Curr Biol 9 (1999) 955-958.
[36] R.G. James, K.A. Bosch, R.M. Kulikauskas, et al., Protein kinase PKN1 represses Wnt/beta-catenin signaling in human melanoma cells, J Biol Chem 288 (2013) 34658-34670.
[37] M. Standaert, G. Bandyopadhyay, L. Galloway, et al., Comparative effects of GTPgammaS and insulin on the activation of Rho, phosphatidylinositol 3-kinase, and protein kinase N in rat adipocytes. Relationship to glucose transport, J Biol Chem 273 (1998) 7470-7477.
[38] P. Moreno-Layseca, J. Icha, H. Hamidi, et al., Integrin trafficking in cells and tissues, Nat Cell Biol 21 (2019) 122-132.
[39] P. Tiwari, A. Mrigwani, H. Kaur, et al., Structural-Mechanical and Biochemical Functions of Classical Cadherins at Cellular Junctions: A Review and Some Hypotheses, Advances in experimental medicine and biology 1112 (2018) 107-138.
[40] E. Calautti, M. Grossi, C. Mammucari, et al., Fyn tyrosine kinase is a downstream mediator of Rho/PRK2 function in keratinocyte cell-cell adhesion, J Cell Biol 156 (2002) 137-148.
[41] C.A. Jilg, A. Ketscher, E. Metzger, et al., PRK1/PKN1 controls migration and metastasis of androgen-independent prostate cancer cells, Oncotarget (2014).
[42] J. Kohler, G. Erlenkamp, A. Eberlin, et al., Lestaurtinib inhibits histone phosphorylation and androgen-dependent gene expression in prostate cancer cells, PLoS One 7 (2012) e34973.

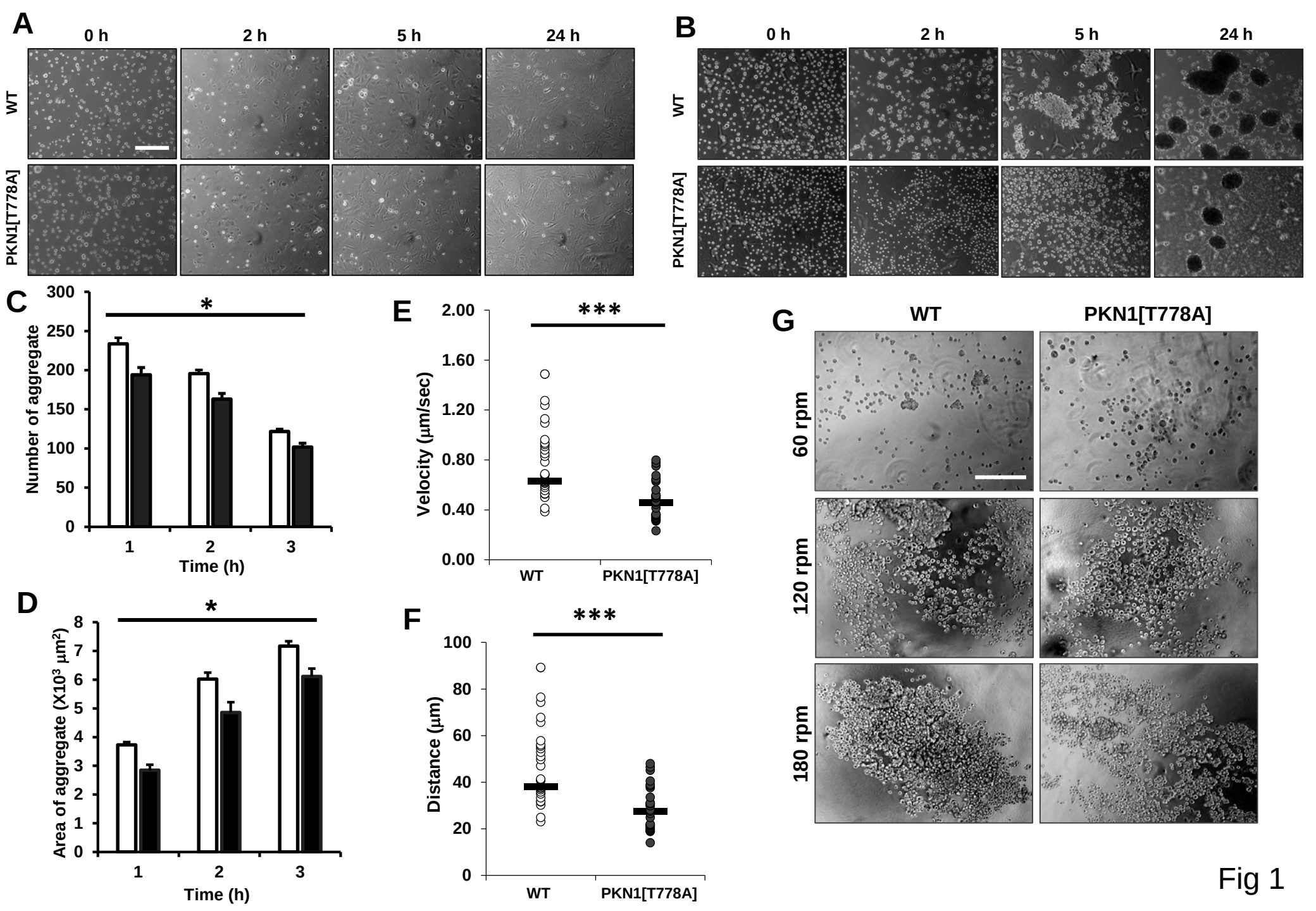
A
0 h
2 h
5 h
24 h
WT
PKN1[T778A]
B
0 h
2 h
5 h
24 h
WT
PKN1[T778A]
C
Number of aggregate
300
250
200
150
100
50
0
*
1
2
3
Time (h)
D
Area of aggregate (X10³ μm²)
8
7
6
5
4
3
2
1
0
*
1
2
3
Time (h)
E
Velocity (μm/sec)
2.00
1.60
1.20
0.80
0.40
0.00
***
WT
PKN1[T778A]
F
Distance (μm)
100
80
60
40
20
0
***
WT
PKN1[T778A]
G
WT
PKN1[T778A]
60 rpm
120 rpm
180 rpm

Fig 1

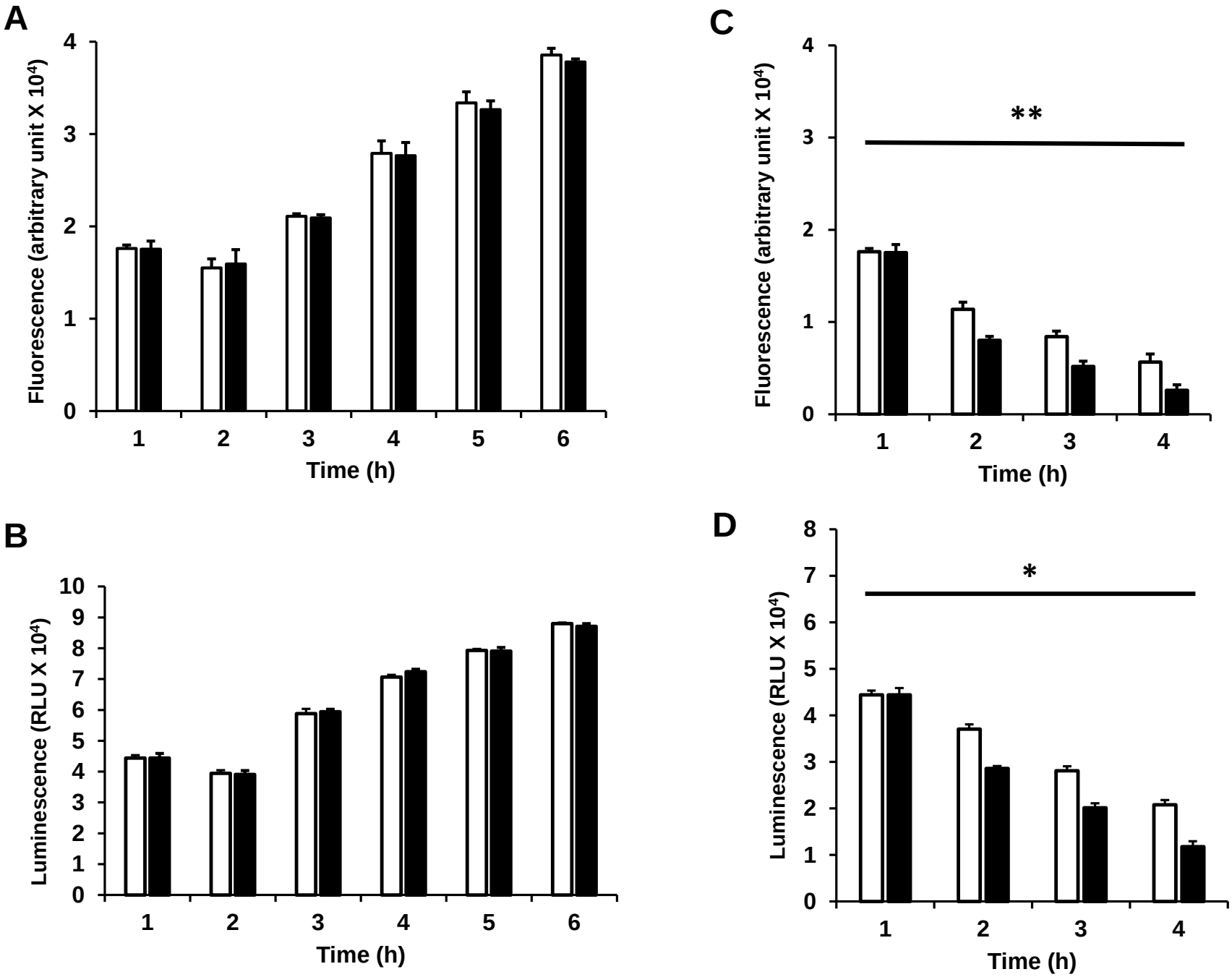
A
Fluorescence (arbitrary unit X 10⁴)
0
1
2
3
4
1
2
3
4
5
6
Time (h)
C
Fluorescence (arbitrary unit X 10⁴)
**
0
1
2
3
4
1
2
3
4
Time (h)
B
Luminescence (RLU X 10⁴)
0
1
2
3
4
5
6
7
8
9
10
1
2
3
4
5
6
Time (h)
D
Luminescence (RLU X 10⁴)
*
0
1
2
3
4
5
6
7
8
1
2
3
4
Time (h)

Fig 2

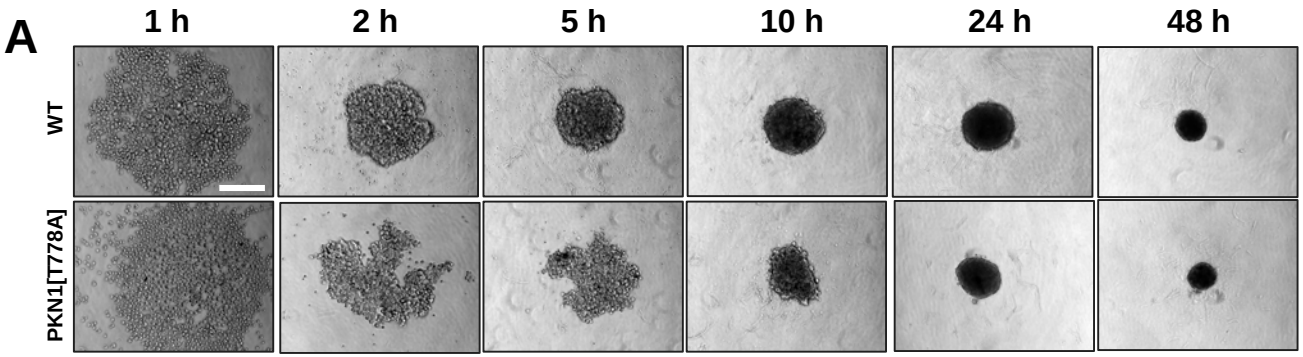
A
1 h
2 h
5 h
10 h
24 h
48 h
WT
PKN1[T778A]

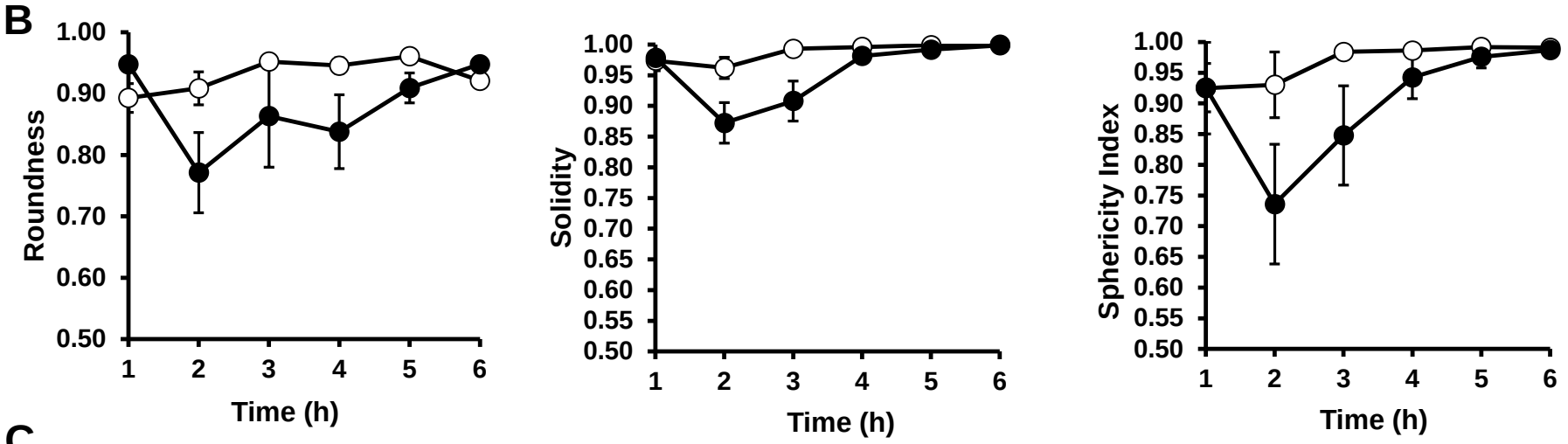
B
Roundness
1.00
0.90
0.80
0.70
0.60
0.50
1
2
3
4
5
6
Time (h)
Solidity
1.00
0.95
0.90
0.85
0.80
0.75
0.70
0.65
0.60
0.55
0.50
Time (h)
Sphericity Index
Time (h)

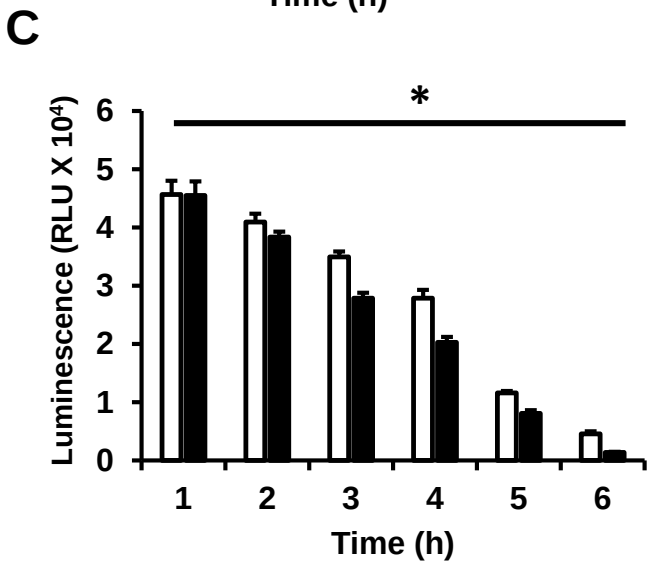
C
*
Luminescence (RLU X 10⁴)
6
5
4
3
2
1
0
1
2
3
4
5
6
Time (h)

Fig 3

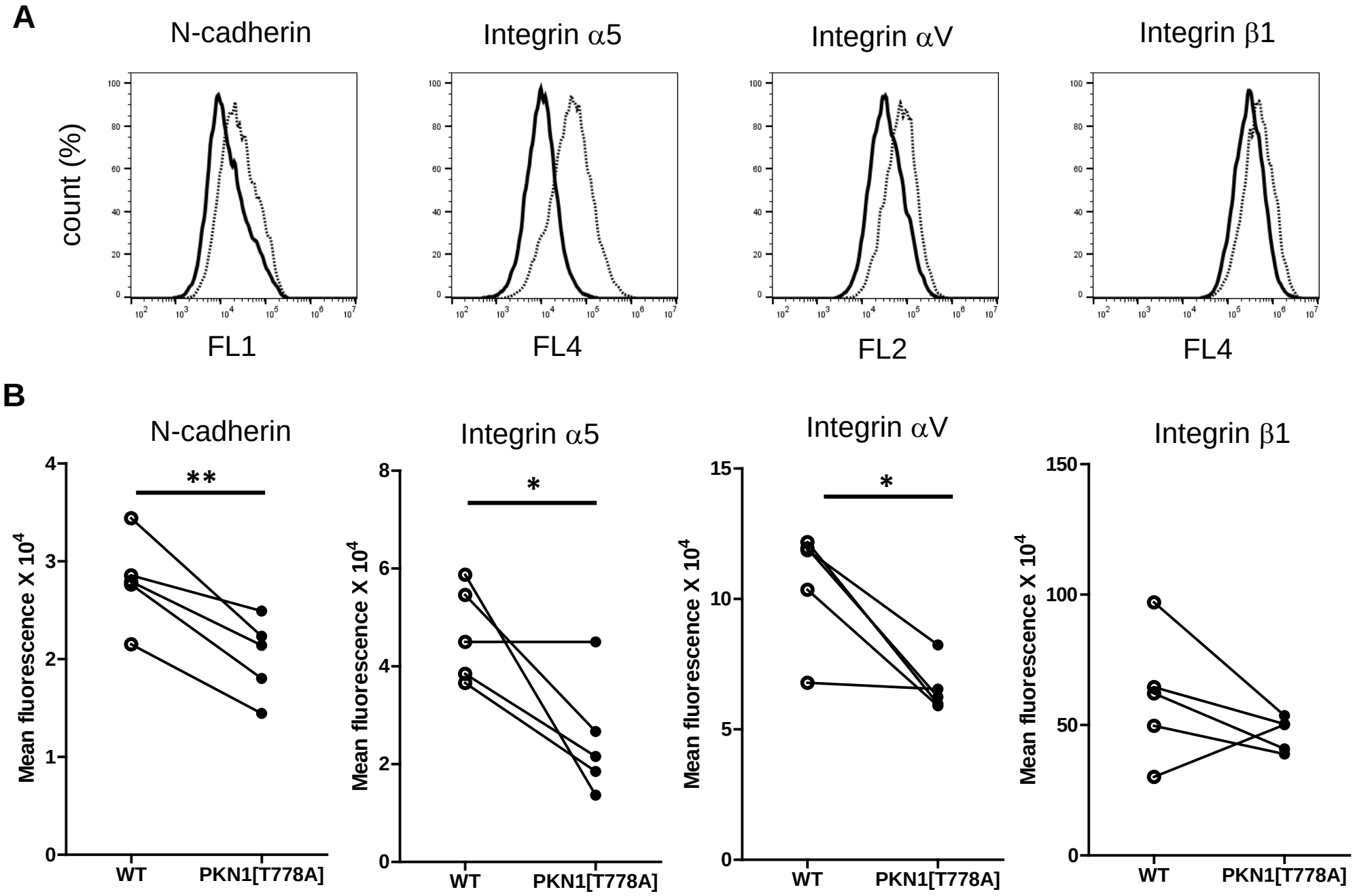
A
N-cadherin
Integrin α5
Integrin αV
Integrin β1
count (%)
FL1
FL4
FL2
FL4
B
N-cadherin
Integrin α5
Integrin αV
Integrin β1
Mean fluorescence X 10^4
**
*
*
WT
PKN1[T778A]